ARMY RESEARCH LABORATORY

Two-Photon Induced Fluorescence and Lasing of Microdroplets (U)

By James B. Gillespie
Battlefield Environment Directorate

Richard K. Chang
Alfred S. Kwok
Yale University

ARL-TR-815

August 1995

19960717 025

Approved for public release; distribution is unlimited.

DTIC QUALITY INSPECTED 1

NOTICES

Disclaimers

The findings in this report are not to be construed as an official Department of the Army position, unless so designated by other authorized documents.

The citation of trade names and names of manufacturers in this report is not to be construed as official Government indorsement or approval of commercial products or services referenced herein.

Destruction Notice

When this document is no longer needed, destroy it by any method that will prevent disclosure of its contents or reconstruction of the document.

REPORT DOCUMENTATION PAGE

Form Approved
OMB No. 0704-0188

1. AGENCY USE ONLY (Leave blank)	2. REPORT DATE	3. REPORT TYPE AND DATES COVERED
	August 1995	Final

4. TITLE AND SUBTITLE

Two-Photon Induced Fluorescence and Lasing of Microdroplets

5. FUNDING NUMBERS

6. AUTHOR(S)

James B. Gillespie (BED)

Richard K. Change and Alfred·S. Kwok (Yale University)

7. PERFORMING ORGANIZATION NAME(S) AND ADDRESS(ES)

U.S. Army Research Laboratory

Battlefield Environment Directorate

Attn: AMSRL-BE-E

White Sands Missile Range, NM 88002-5501

8. PERFORMING ORGANIZATION REPORT NUMBER

ARL-TR-815

9. SPONSORING/MONITORING AGENCY NAME(S) AND ADDRESS(ES)

U.S. Army Research Laboratory

2800 Powder Mill Road

Adelphi, MD 20783-1145

10. SPONSORING/MONITORING AGENCY REPORT NUMBER

ARL-TR-815

11. SUPPLEMENTARY NOTES

12a. DISTRIBUTION/AVAILABILITY STATEMENT

Approved for public release; distribution is unlimited.

12b. DISTRIBUTION CODE

A

13. ABSTRACT (Maximum 200 words)

The feasibility of using two-photon induced fluorescence of amino acids is examined for its potential as a detection technique for biological aerosols. The research was motivated by the problem of spectral discrimination encountered in fluorescence applications. Two separate experiments were performed: 1) two-photon induced fluorescence of the three aromatic amino acids and 2) two-photon pumped lasing in spherical droplets doped with rhodomine 6g dye. It was found in the first experiment that there is greater specificity for two-photon fluorescence than for one-photon induced fluorescence; however, the effect is very weak. The lasing experiment indicated that lasing is intense, but there can only be a short distance from the source to the droplet.

14. SUBJECT TERMS

ultraviolet, flourescence, two-photon, amino acid

15. NUMBER OF PAGES

54

16. PRICE CODE

17. SECURITY CLASSIFICATION OF REPORT	18. SECURITY CLASSIFICATION OF THIS PAGE	19. SECURITY CLASSIFICATION OF ABSTRACT	20. LIMITATION OF ABSTRACT
Unclassified	Unclassified	Unclassified	SAR

NSN 7540-01-280-5500

Standard Form 298 (Rev. 2-89)
Prescribed by ANSI Std. Z39-18
298-102

Contents

Figures

2

Executive Summary

Remote chemical sensing of biological material suspended in the atmosphere is of vital interest to the Army. It is recognized that a remote sensing system, based on laser induced fluorescence of biological agents, offers the greatest potential for success. However, fluorescence has a fundamental limitation; the fluorescence emission spectra of most substances are broad and featureless, which leads to a serious problem of identification. Another problem, energy transfer in the fluorescence process, occurs when several substances are in the same droplet, such as the aromatic amino acids: tryptophan, tyrosine, and phenylalanine. In such a situation, the molecules absorb the exciting photons, but only one of the substances will fluoresce because the others transfer their energy to it. In the case of amino acids, only the fluorescence from the tryptophan is generally observed. To overcome the lack of specificity of fluorescence, we have considered the potential of two-photon excited fluorescence. This technique is very weak, but could potentially produce enough specificity if only one excitation wavelength is available.

To evaluate this technique, we performed two sets of experiments: (1) two-photon excitation (TPE) and fluorescence of the three amino acids (tryptophan, tryrosine, and phenylalanine) and (2) two-photon pumped lasing in spherical droplets doped with rhodamine 6G dye. The TPE of the aromatic amino acids demonstrated that all three acids could be observed simultaneously, and in some instances, the two-photon fluorescences for phenylalanine and tyrosine were stronger than for tryptophan. The two-photon induced fluorescence of the amino acids indicated that this technique has the potential for greater specificity in the detection of biological materials. Further research is necessary before a full evaluation of the potential for near-field remote sensing of biological agents can be made. Three conclusions can be drawn from the two-photon induced lasing: (1) fluorescence is intense even for TPE, (2) the two-photon pumping should be into a specific electronic band, and (3) degenerate factors that work against the build up of lasing are not so dominant as to prevent lasing.

1. Introduction

Fluorescence has been demonstrated as a practical technique for remote sensing of trace species. Because the electromagnetic waves are propagating in air, the absorption and fluorescence bands of the species must not have photon energies greater than 6.8 eV or wavelengths shorter than 186 nm. Ideally the fluorescence emission should occur between 250 and 300 nm, because in this wavelength region, the spectral radiance from the sun is very low, and solar-blind detectors with high quantum efficiencies can be used. In the region between 186 and 250 nm, there is some atmospheric propagation, but oxygen becomes a strong absorber below 250 nm, and significant detection ranges are difficult to obtain if the wavelength is much below 250 nm. With one-photon excitation (OPE) of fluorescence, the emission is nearly always red shifted from the pump-laser wavelength; therefore, it is the atmospheric attenuation of the laser wavelength that limits the range. Even for wavelengths longer than 250 nm, there can be significant atmospheric attenuation if the visibility is low. With two-photon excitation (TPE) of fluorescence, the emission is blue shifted from the pump-laser wavelength. Blue shifting ensures significantly less attenuation of the laser beam by the atmosphere.

2. Background

2.1 Fluorescence

Fluorescence is a process in which an atom or a molecule absorbs a photon and is excited from the electronic ground state to a higher electronic state. The atom or molecule undergoes nonradiative emission of energy to the lowest vibrational state in the first electronic state. The atom or molecule radiatively decays from the first electronic state to one of the vibrational levels of the electronic ground state and nonradiatively decays to the lowest vibrational state in the electronic ground state. This results in a fluorescence photon with less energy than the exciting photon; thus, a longer wavelength (sometimes referred to as red or Stokes shifted). This process usually takes about a few nanoseconds. Because the fluorescence emission can occur at any of the vibrational levels of the first electronic ground state, a fluorescence emission spectrum of a substance is generally broad and somewhat featureless. The efficiency of this process varies greatly from substance to substance and will vary with the wavelength of excitation. This efficiency, generally, is referred to as the photon yield and is dependent on the fluorescence cross section. TPE occurs when an atom or molecule has absorbed one photon, then absorbs another before it has had time (less than the decay time of the molecule) to decay. This sometimes results in a transition into a higher electronic state—a state quite often only reached by vacuum ultraviolet (VUV) excitation. This can result in observation of spectral features not seen in OPE, especially if several fluorescing species are present in the same sample. The main disadvantage of TPE is the requirement for high-intensity laser pulses, because the effective absorption coefficient α_{eff} is the product of the two-photon absorption (TPA) coefficient β (in units of cm/MW) and the input laser intensity I_{input} (in units of MW/cm^2) ($\alpha_{eff} = \beta I_{input}$ (in units of cm^{-1})). The one-photon absorption (OPA) coefficient α (in units of cm^{-1}) is well tabulated in terms of absorption values and in spectral locations of the OPA bands. By contrast, the absolute absorption values and spectral locations of the two-photon bands are usually unknown for most substances.

2.2 Atmospheric Effects

The atmosphere affects fluorescence remote sensing in three ways: (1) extinction of the laser beam, resulting in much less energy incident on the sample volume; (2) extinction of the return fluorescence emission spectrum, perhaps altering the spectral signature of the return signal; and (3) quenching, a process in which molecules that are excited undergo collisions with oxygen molecules and transfer their excess energy to the oxygen so fluorescence does not occur. Atmospheric quenching usually prevents fluorescence detection of gases in the troposphere, and we are concerned with aerosols; therefore, this aspect is not relevant and will not be considered further. The atmospheric extinction consists of molecular absorption and scattering and aerosol absorption and scattering. These effects become much more severe as the wavelength becomes shorter. Ozone and oxygen are the two primary absorbing molecular species in the atmosphere, and atmospheric dust is the primary source of extinction for wavelengths from visible down to 250 nm. For OPE, an ultraviolet (UV) laser is usually required. This source is usually limited in range by the strong atmospheric attenuation. For TPE, a visible laser can be used, resulting in transmission of significantly more energy to the remote sample volume. This is probably the most significant advantage of TPE.

For this investigation, we performed two separate, distinct experiments: (1) we examined TPE of amino acids in microdroplets, and (2) we examined TPE induced lazing of dye doped microdroplets. These experiments will be discussed in turn below.

3. Results

3.1 Amino Acids

Because the aromatic amino acids are present in most biological agents, their TPE fluorescence characteristics are studied to determine the feasibility of using TPE spectroscopy as a means of remote sensing of biological agents.

3.1.1 Review of One-Photon Fluorescence Spectra

The OPA and fluorescence spectra of the aromatic amino acids are well documented. The amino acids absorb light at longer wavelengths than the nonaromatics because the π^* excitation bands of the aromatic chromophore are lower than the excitation bands of the nonaromatics. Figure 1 shows the absorption spectra of tryptophan, tyrosine, and phenylalanine from 190 to 310 nm. [1] A logarithmic scale of the molar absorptivity is used to emphasize the weak absorption peak for wavelengths longer than 230 nm.

Tyrosine and phenylalanine contain a benzene ring in their functional group; therefore, they have similar spectral patterns. In fact, their electronic states resemble that of the parent benzene molecule. For spectroscopic purposes, tyrosine and phenylalanine can be considered benzene molecules with an alanyl substitution for phenylalanine and an alanyl plus hydroxyl substitution for tyrosine. The first electronic state of benzene is labelled the L_b state (Platt notation) or the B_{2u} state (group theory notation). The benzene molecule has a D_{6h} point group. The electric dipole operator transforms as the irreducible representation E_{1u} of D_{6h}. Therefore, one can show with group theory that the unassisted OPA transition from the A_{1g} ground state to the B_{2u} state is strictly forbidden. The fact that the one-photon transition or absorption can be observed in benzene is due to vibronic coupling with the υ_6 vibration, which gives rise to a progression in the OPA spectrum of benzene starting at 255 nm.

In tyrosine and phenylalanine, the symmetry of the benzene ring is broken by the alanyl substitution and by the alanyl plus a hydroxyl substitution, respectively. Consequently, the lack of inversion symmetry in tyrosine and
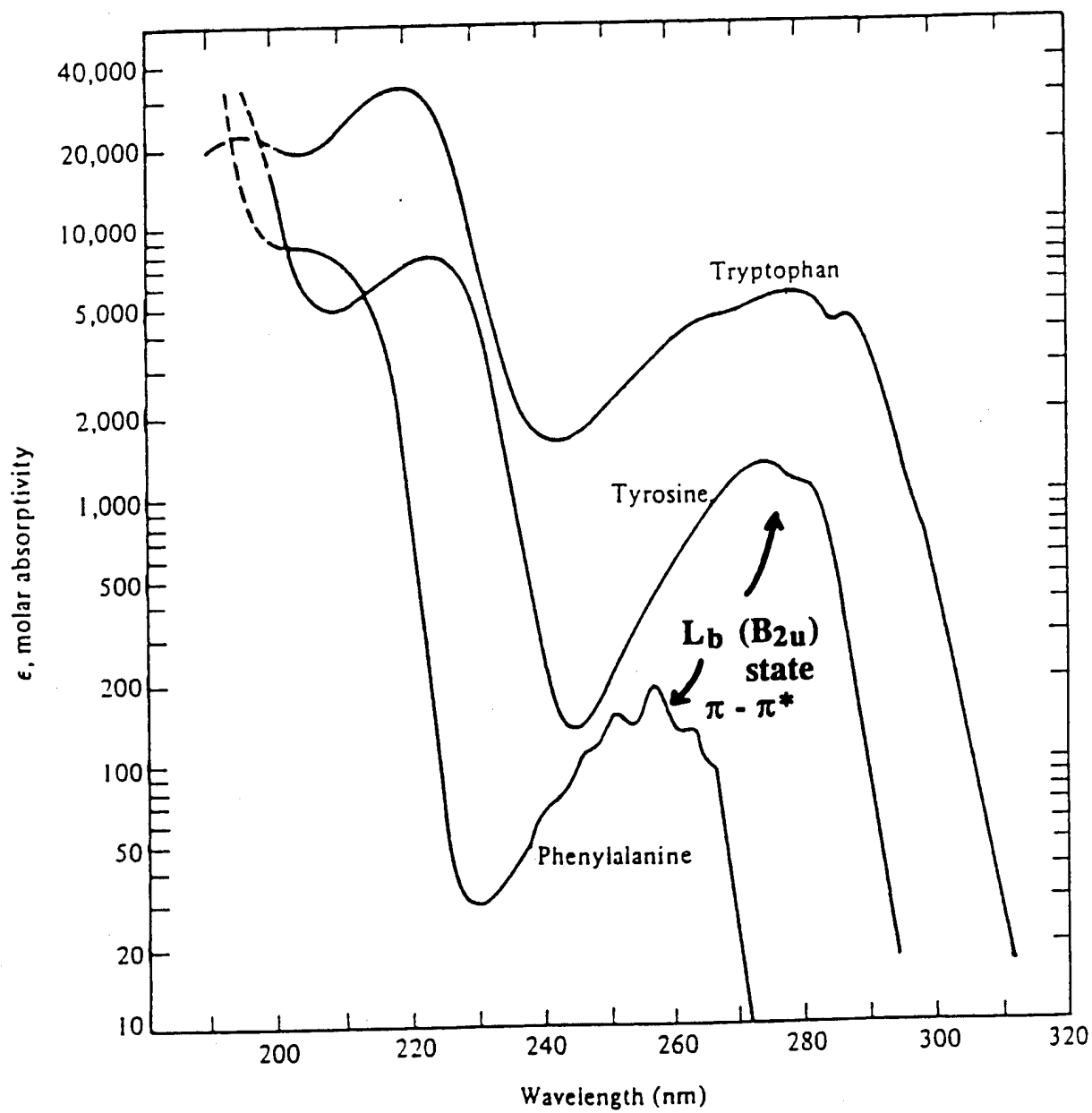
9

Figure 1. Absorption spectra in the UV of aromatic amino acids (tryptophan, tyrosine, and phenylalanine) at a pH of 6.

phenylalanine gives rise to a Franck-Condon allowed progression in the OPA spectrum. For OPA, the affect of the hydroxyl substitution in phenylalanine is much stronger than the alanyl substitution in tyrosine and the υ_6 vibronic coupling in benzene. Therefore, the molar absorptivity of tyrosine is almost an order of magnitude stronger than that of phenylalanine, which in turn is stronger than the molar absorptivity of benzene. [2]

Tryptophan contains an indole (five-membered ring) in its functional group, and it has a broad absorption peak extending from 240 to 300 nm, caused by a mixture of the L_a and L_b states of the indole. Extensive calculations were performed to match the observed OPA and TPA peaks (position and strength) with the perturbed (vibronic and substitutional) benzene and indole molecular orbitals of this energy region. [2,3,4]

Figure 2 shows that further into the UV the following absorption peaks exist: [1] for tyrosine, peaks at about 224 and 192 nm; and for phenylalanine, peaks at about 206 (more like a shoulder) and 187 nm. The peaks correspond to the second higher excited L_a state (or B_{1u} group theory notation of benzene) at 205 nm and to the third higher excited $B_{a,b}$ state (E_{1u} in group theory notation of benzene) at 185 nm, as well as the excited state of the carboxylate group. The spectral positions of the absorption and fluorescence peaks are affected by substitutional groups of the aromatic amino acids. [5] In benzene, dipole transition from the A_{1g} ground state to the B_{1u} state is partially allowed because of vibronic coupling in benzene and substitutional effects in the amino acids. Dipole transition from the A_{1g} state to the E_{1u} state of benzene is allowed; therefore, dipole is allowed for the amino acids. For tryptophan, the absorption peaks at 220 and 197 nm are associated with the higher excited states of the indole. Because the strength of the UV absorption peak at 220 nm, it is believed that this peak involves one-photon allowed dipole transitions.

Figure 3 shows the fluorescence spectra of the three aromatic amino acids obtained with the excitation of the 253.7 nm mercury lamp. [6] Most notable is the fluorescence of tryptophan, approximately 15 percent of which lies at fluorescence wavelength $\lambda > 400$ nm, giving tryptophan solution a deep purple glow under UV excitation. The fluorescence yield of the three aromatic amino acids were studied in solutions of different pHs. At pH +7, tryptophan and
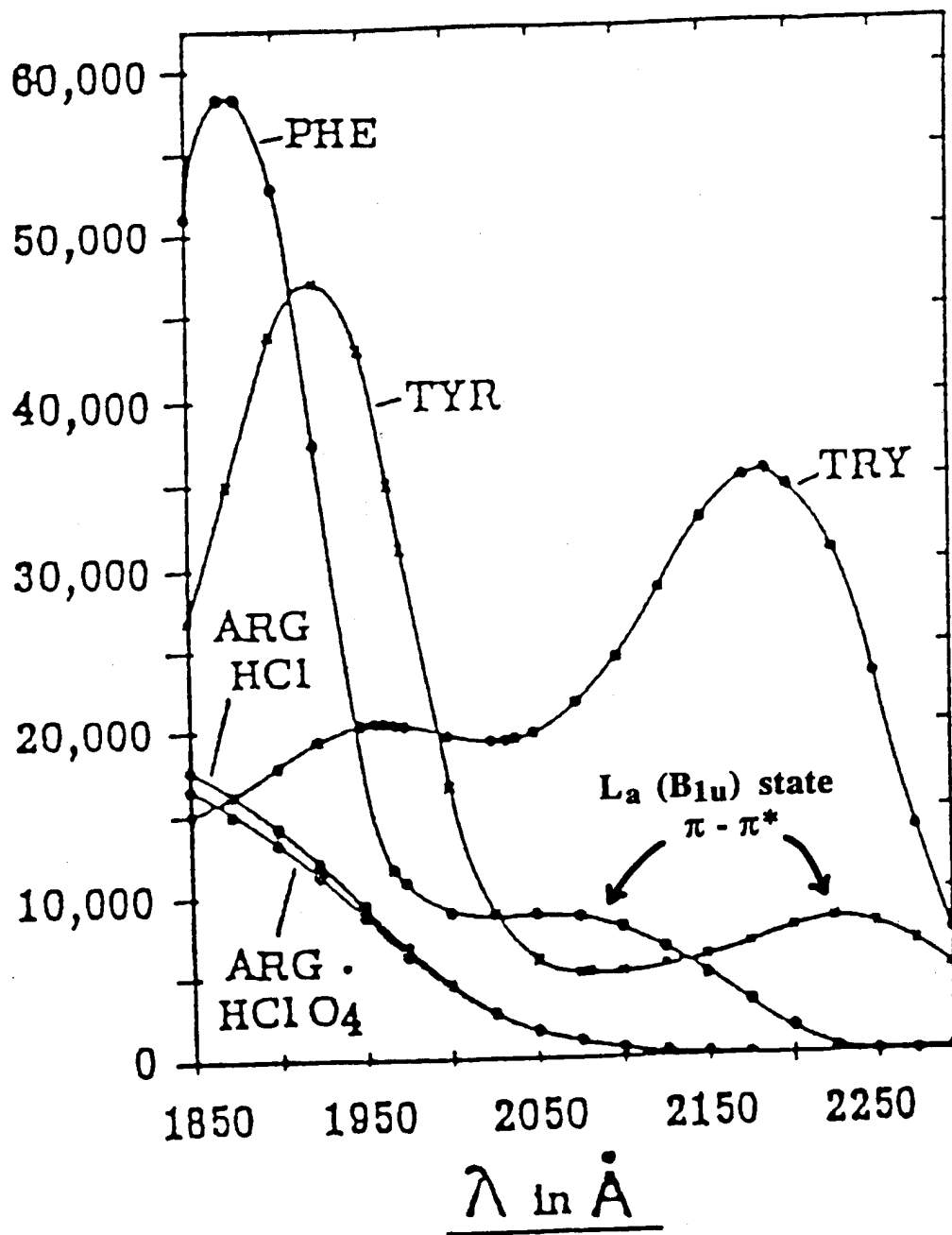
Figure 2. Absorption spectra of aromatic amino acids further in the UV.
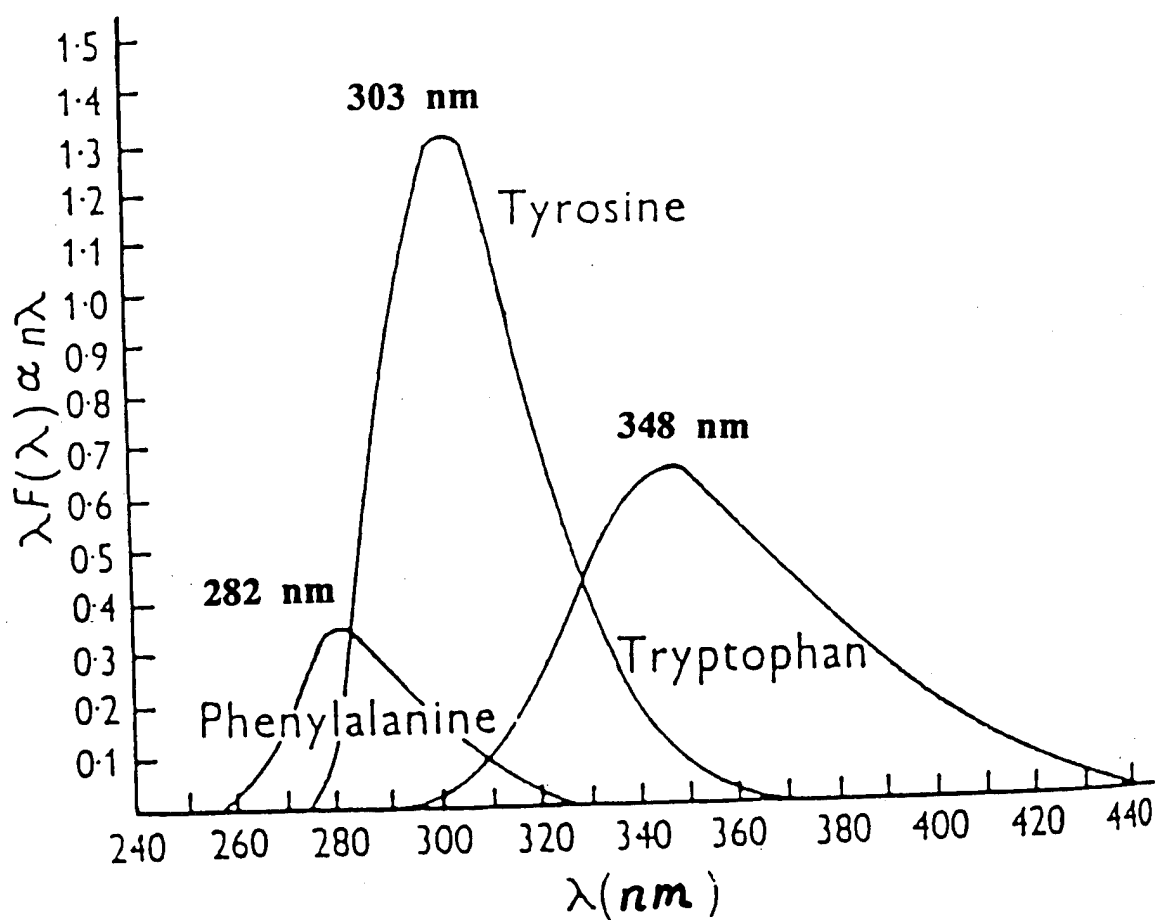
Figure 3. Fluorescence spectra of the aromatic amino acids in water. The ordinate is relative fluorescence intensity, and the abscissa is wavelength.

tyrosine have similar quantum yields (13 to 14 percent). However, the fluorescence quantum yield of phenylalanine is about six times less. [7] The combination of low fluorescence quantum yield and low absorption cross section into the first excited state (L_b band) makes phenylalanine hard to distinguish in the presence of lower concentrations of tryptophan or tyrosine with the OPE/fluorescence technique.

3.1.2 Review of Two-Photon Spectra

TPA and fluorescence spectra of the less studied aromatic amino acids have been limited to incident excitation wavelengths $\lambda_{inc} = 440$ to 600 nm (a wavelength region in which TPE can access the L_b (B_{2u}) band of benzene and the overlapping L_a and L_b bands of indole) (figure 4). [8] For benzene, two-photon transition from the ground A_{1g} to B_{2u} band is strictly forbidden, and TPA in benzene occurs through vibronic coupling of the υ_{14} vibration. In the case of OPA, the effect of substitution dominates over vibronic coupling. However, for TPA, vibronic coupling dominates in the two-photon transition into the L_b state. Because vibronic coupling dominates in tyrosine, phenylalanine, and benzene, these species should have nearly the same TPA cross section for transitions into the L_b band. [9,10] The estimated TPA cross section for phenylalanine, tyrosine, and tryptophan is discussed in previous research. [10] Figure 4d shows that the relative TPE fluorescence signal of tryptophan with λ_{inc} in the 500- to 560-nm range is an order of magnitude higher than that of tyrosine and phenylalanine. The larger TPE fluorescence is indicative of a symmetry allowed two-photon transition or absorption into the L_b and L_a bands for tryptophan. The further increase in TPE fluorescence intensity with $\lambda_{inc} < 480$ nm is probably due to two-photon transition to the next higher band, the L_a (B_{1u}) band.

3.1.3 Experimental Results and Discussion

For this work we investigated the TPE fluorescence of the aromatic amino acids with $\lambda_{inc} < 440$ nm. Samples of L-tyrosine, L-phenylalanine, and L-tryptophan were obtained from Sigma Corporation and used without further purification. Aqueous solutions containing 10^{-3} M of the amino acids were made using deionized water.

14

Figure 4. TPE and OPE spectra of the fluorescence emission from aromatic amino solutions: (a) phenylalanine, (b) tyrosine, (c) tryptophan. The relative TPE spectra of the fluorescence intensity is shown in (d).
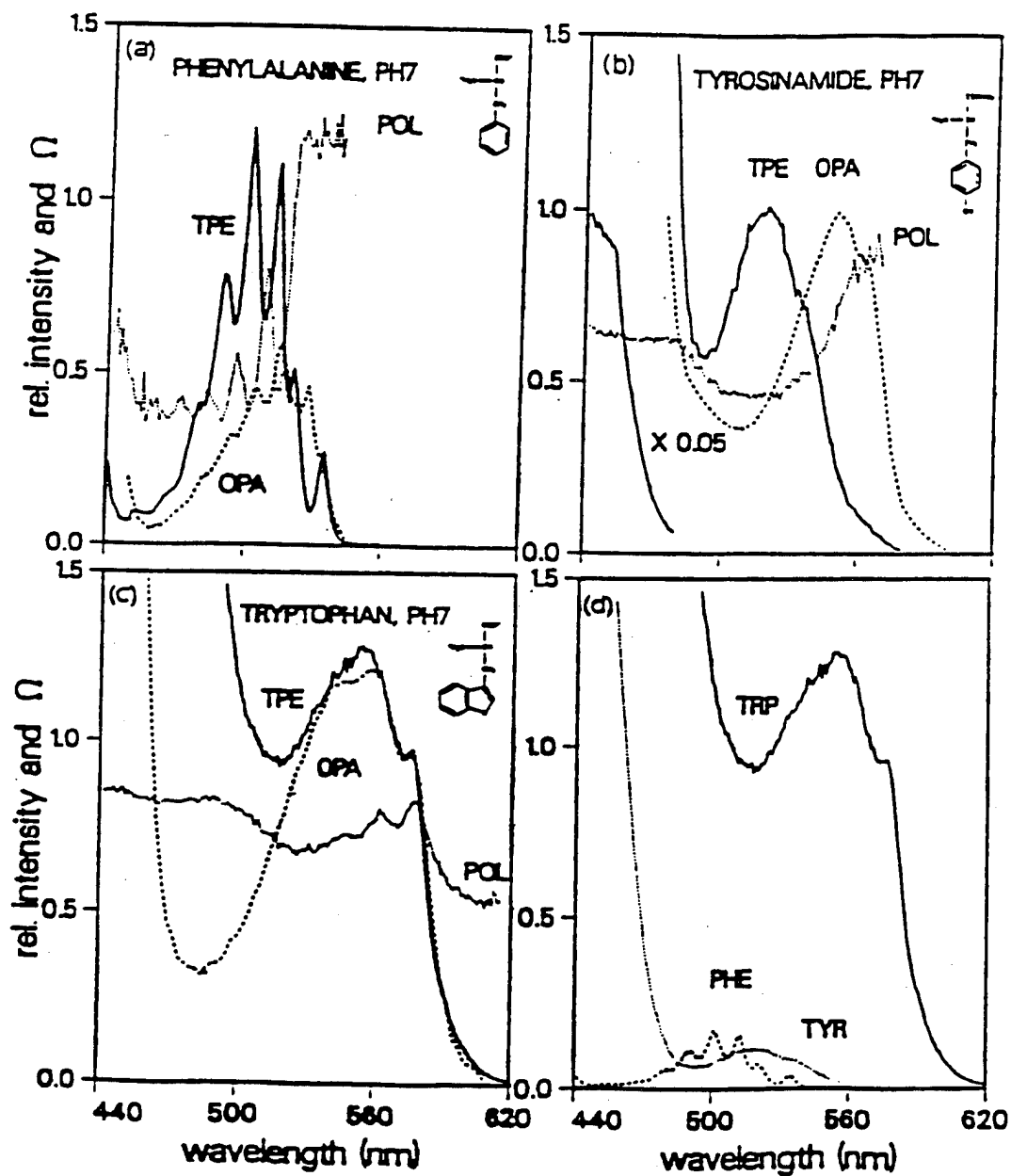
15

Figure 5 shows the experimental setup. The excitation source is a Lambda-Physik model LPD 3000 tunable dye laser pumped by a Lumonics model HyperEx-400 excimer laser operating at 308 nm and 10-Hz pulse repetition rate. The dye laser beam is spatially filtered to produce a 3-mm diameter Gaussian beam focused by a 17-cm focal length lens into a 1- by 3-cm quartz cell with a beam spot size of about 20 μm. The laser intensity is varied by rotating the axis of a first Glan-Taylor prism with respect to another Glan-Taylor prism, the axis of which is fixed. The laser intensity is monitored at every incident wavelength λ_{inc} by a photodiode (the quartz cell is removed during this step). The fluorescence from the amino acid is collected at 90° to the incident laser by a pair of quartz lenses (f/1) and focused into a solar-blind photomultiplier tube (PMT) (Hammamatsu model 166UH). A solar-blind PMT is suitable for remote sensing as it has a high rejection ratio for visible light. A band-pass filter (Shott UG11) placed in front of the solar-blind PMT reduces the wavelength unshifted scattered laser light from a level that saturates the PMT to a negligible level (transmission of UG11 at λ_{inc} is less than 10^{-5}). The output of the PMT is directly connected to the 50-Ω input of a 250-MHz digital oscilloscope (Tektronix model 2431L). Because the oscilloscope can only sample every 4 ns, and the fluorescence only lasts about 20 ns, it is operated in the repetitive mode such that 20 input pulses are sampled for an acquisition. The display is averaged over four acquisitions.

To ensure that the apparatus is functioning and the sample amino acids had the necessary purity, we remeasured the TPE fluorescence spectra of the aromatic amino acids in the region of λ_{inc} = 490 to 565 nm to compare our results with published results. [8] The laser dye coumarin 307 was used for varying the excitation wavelength from 490 to 530 nm, and coumarin 540A was used for varying the excitation from 534 to 564 nm. Instead of using the usual procedure of dividing the detected intensity of the two-photon fluorescence by the input laser intensity, we opted to keep the input laser intensity fixed with the variable attenuator formed by the pair of Glan-Taylor prisms. As the λ_{inc} is tuned, we directly plot the two-photon fluorescence intensity and display the TPE profile. The resultant TPE fluorescence from each amino acid is not spectrally analyzed by a spectrometer but must first pass a UG11 filter before detection by the solar-blind PMT. The small amount of unavoidable TPE fluorescence intensity from the quartz cell and impurities in the deionized water

16
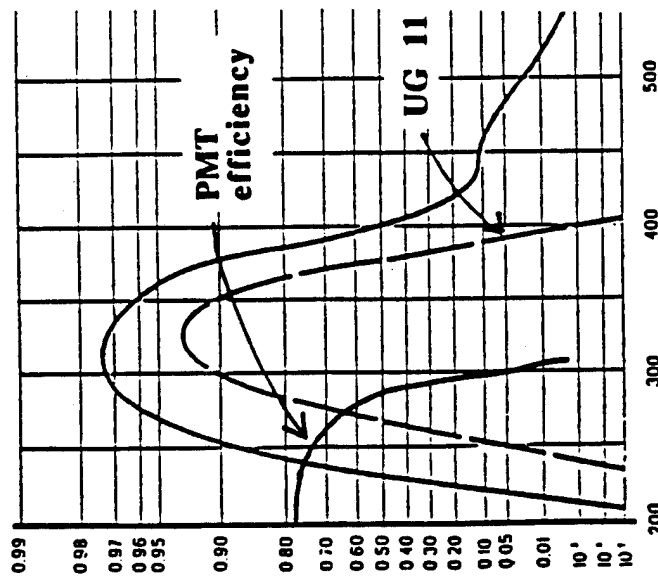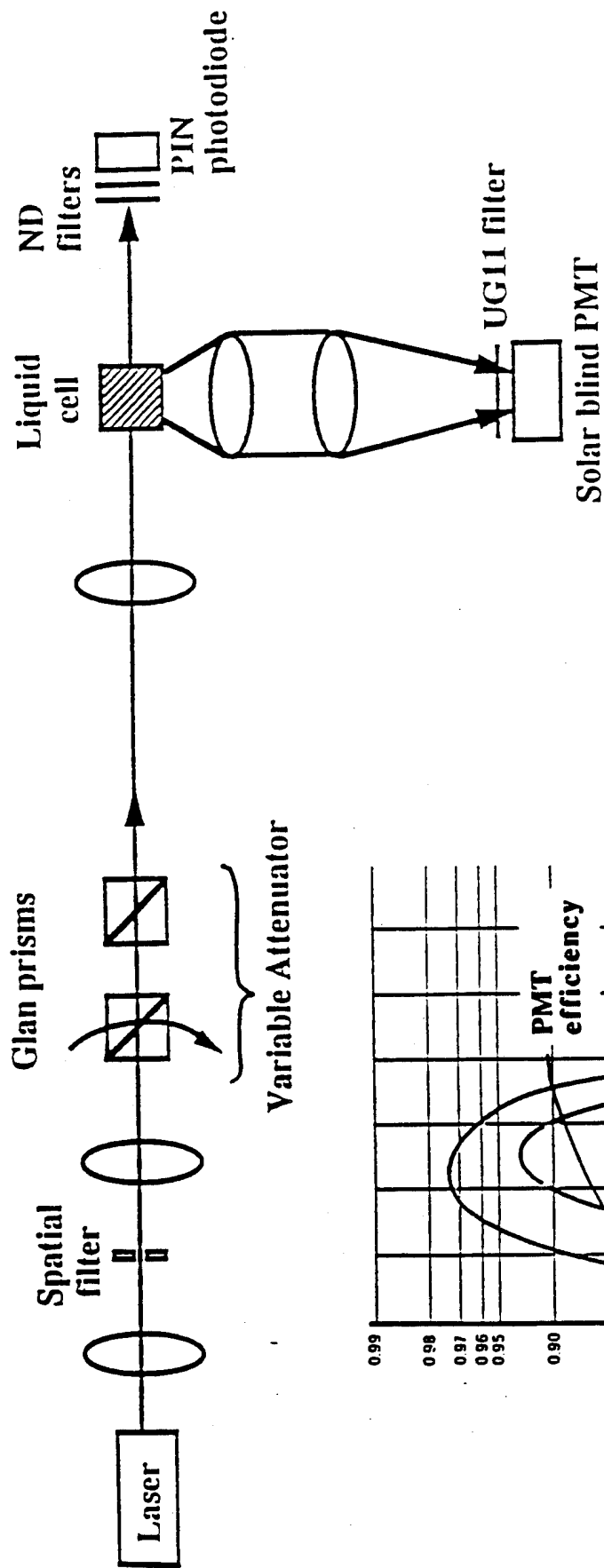
Figure 5. Experimental setup. The photo response of the solar-blind PMT and the transmission of the UG11 glass filter.

is first detected with the quartz cell containing only deionized water and is subtracted from the TPE fluorescence intensity from the quartz cell containing 10^{-3} M of one of the three types of amino acid in deionized water.

Figure 6 shows the TPE spectrum with λ_{inc} tuned from 490 to 530 nm. Each laser pulse contains about 0.17 mJ and reaches an input intensity of about 3 GW/cm^2. For each comparison with the published results, [8] the inset of figure 6 is the TPE spectrum and published TPE spectra are attributed to the photo response of the solar-blind PMT used in this experiment.

The photo response of the solar-blind PMT is greatly reduced for wavelengths longer than 300 nm (figure 5). Because 95 percent of the tryptophan fluorescence wavelength is longer than 300 nm, the TPE fluorescence signal of tryptophan is drastically reduced relative to that of tyrosine and phenylalanine. Similarly, the tyrosine and phenylalanine fluorescence spectra have fluorescence emissions greater than 300 nm. Lesser portions of the tyrosine and phenylalanine fluorescence have emissions greater than 300 nm, (only about 60 percent for tyrosine and 30 percent for phenylalanine) (figure 3). When the solar-blind PMT is used and λ_{inc} is tuned from 490 to 540 nm, the weakest TPE fluorescence intensity is from tryptophan. Without the solar-blind PMT, the TPE fluorescence intensity is totally dominated by tryptophan (figure 4d). With the solar-blind PMT, there is a possibility of detecting the fluorescence signal from amino acids other than tryptophan.

By using the solar-blind PMT, the strongest TPE fluorescence intensity is from tyrosine when λ_{inc} is tuned from 540 to 565 nm, and the strongest TPE fluorescence intensity is from phenylalanine when λ_{inc} is tuned from 490 to 520 nm. There is an optimal wavelength region to detect tyrosine and phenylalanine with the solar-blind PMT.

In figure 6 the discontinuity, at 530 and 534 nm, between the two sets of TPE data points is an artifact of being at the edge of the tuning range of the two different laser dyes. The laser pulse shape at the edge of the dye tuning range can differ from that at the center of the dye tuning range. Pulse change is particularly prominent at the ends of the tuning range. Thus, even when the laser pulse energies are the same at the two wavelengths, a pulse shape change can lead to a peak intensity change that can cause a change in the peak two-photon fluorescence intensity.

18

TPE Spectra of Aqueous Aromatic Amino Acid Solutions

Figure 6. The TPE spectra of the fluorescence from aqueous solution of the tryptophan (dots), tryrosine (triangles), and phenylalanine (crosses) at 10^{-3} M. The incident laser wavelength extends from 490 to 565 nm.

Our TPE spectrum for tryptophan (solid dots in figure 6) does not show the peak observed in figure 4c at about 545 nm. The lack of TPE peak in our spectra may be attributed to the reduced fluorescence signal detected by the solar-blind PMT. Our TPE spectrum for tyrosine (solid triangles in figure 6) shows a peak at about 525 nm, which agrees with the TPE peak shown in figure 4b. The TPE peak at 525 nm corresponds to TPE from the ground A_{1g} to B_{2u} (L_b). TPE fluorescence from phenylalanine cannot be observed until $\lambda_{inc} < 545$ nm. Our data does not reveal the vibronic related structures observed in the published phenylalanine TPE spectra (figure 4a) because our input wavelength is tuned too coarsely. However, our TPE spectra agree with the general trend displayed in figure 4a.

Our attempt to investigate the TPE spectra of the three aromatic amino acids for $\lambda_{inc} < 440$ nm proved to be more difficult. The neutral density filters placed in front of the photodiode to monitor the input laser intensity are designed for visible wavelength, and their transmission begins to roll off at wavelengths less than 395 nm. Therefore, we were unable to obtain any meaningful TPA spectra for laser incident wavelengths less than 395 nm. The laser dye PBBO was used for incident laser wavelengths in the range of 396 to 408 nm, and Bis-MSD was used for the wavelength range of 414 to 428 nm. The narrow tuning range illustrates another inconvenience working in this blue wavelength region. The TPE fluorescence of tyrosine and phenylalanine in this wavelength region is strong and saturates the PMT when its gain and the input laser intensity are set to the amino acids and when the incident wavelength is in the range of 490 to 564 nm. Therefore, when λ_{inc} is in the range of 396 to 428 nm, the laser intensity is decreased by 50 percent and the PMT gain is reduced by decreasing the high voltage of the power supply. Because the photomultiplier gain is not linear with the input voltage, a quantitative comparison between the fluorescence intensity for the incident laser wavelength in the 490- to 564-nm range cannot be made with that for the 396- to 428-nm range. However, one can roughly estimate that the TPA cross section in the region of incident wavelength of 396 to 408 nm is within an order of magnitude (probably closer to three to five times) of the TPA cross section in the region of $\lambda_{inc} = 490$ to 560 nm. We estimate the TPA cross section to be about 0.5×10^{-50} cm^{4}s.

Figure 7 shows the TPE spectra for the three amino acids in the range of λ_{inc} = 396 to 408 nm. The tryptophan curve (solid circles) remains featureless because of the poor signal-to-noise ratio. The phenylalanine curve (crosses) increases monotonically as 1/2 λ_{inc} approaches the 187-nm peak observed in the one-photon spectra (figure 2) that correspond to transitions from the A_{1g} ground state to the E_{1u} benzene state and the upper excited carboxylate state. The same trend of increase is observed in tyrosine (solid triangles) for λ_{inc} < 410 nm. Two-photon transition to the E_{1u} benzene state is not allowed by the group theory selection rule but becomes allowed if vibrational and substitutional perturbations are included. However, neither this nor the two-photon transition of the carboxylate group were studied. When λ_{inc} < 400 nm, the TPE fluorescence from other substances may also be observed even though the A_{1g} ground state to E_{1u} has a large TPA cross section.

Figure 7 shows that the tyrosine signal also increases from 414 to 428 nm as 1/2 λ_{inc} approaches the B_{1u} state observed in the one-photon spectra (figure 2). An analogous TPE fluorescence increase cannot be observed for phenylalanine (figure 7). A decrease of the TPE fluorescence is noted when λ_{inc} is varied from 414 to 428 nm. It should be noted that the one-photon spectrum associated with transitions into the B_{1u} state appears more like a shoulder in the phenylalanine (figure 2). Two-photon transition to the B_{1u} state is again forbidden by group theory but is allowed through vibronic coupling. Moreover, it has been shown for monosubstituted benzenes that substitutional effects dominate over vibronic effects in two-photon transitions of the next higher B_{1u} state, while the opposite is true for the two-photon transition into the lower B_{2u} state in which the vibronic coupling dominates. [11]

There are several experimental limitations in the research described above; however, there are several main conclusions that we can draw from our study with solar-blind PMT detection of the TPE fluorescence of the three aromatic amino acids:

1. TPE fluorescence for tyrosine and tryptophan are stronger than for phenylalanine with λ_{inc} in the range of 540 to 565 nm.

TPE Spectra of Aqueous Aromatic Amino Acid Solutions

Tyrosine

Phenylalanine

Tryptophan

Intensity (arb. units)
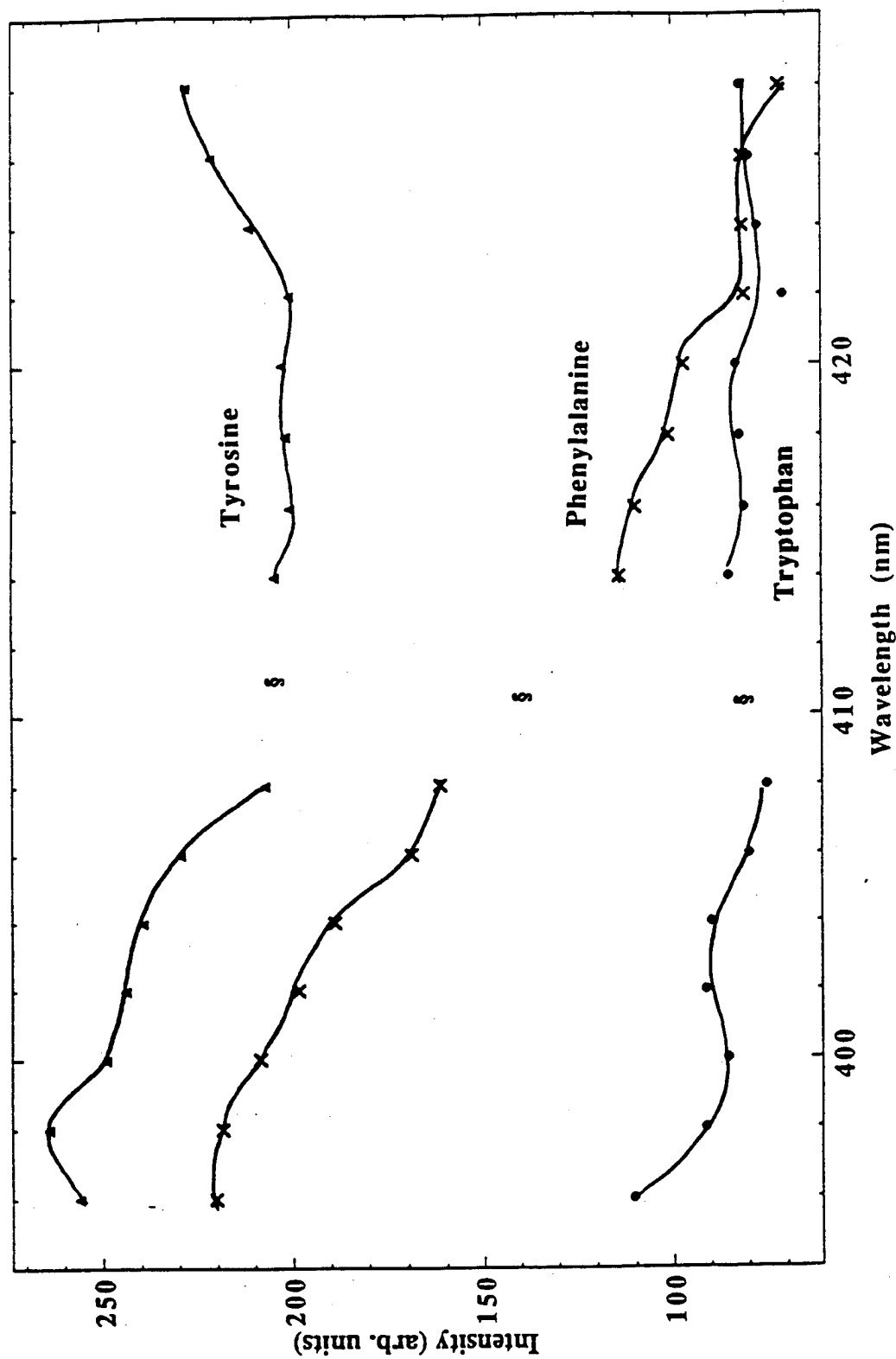
Wavelength (nm)

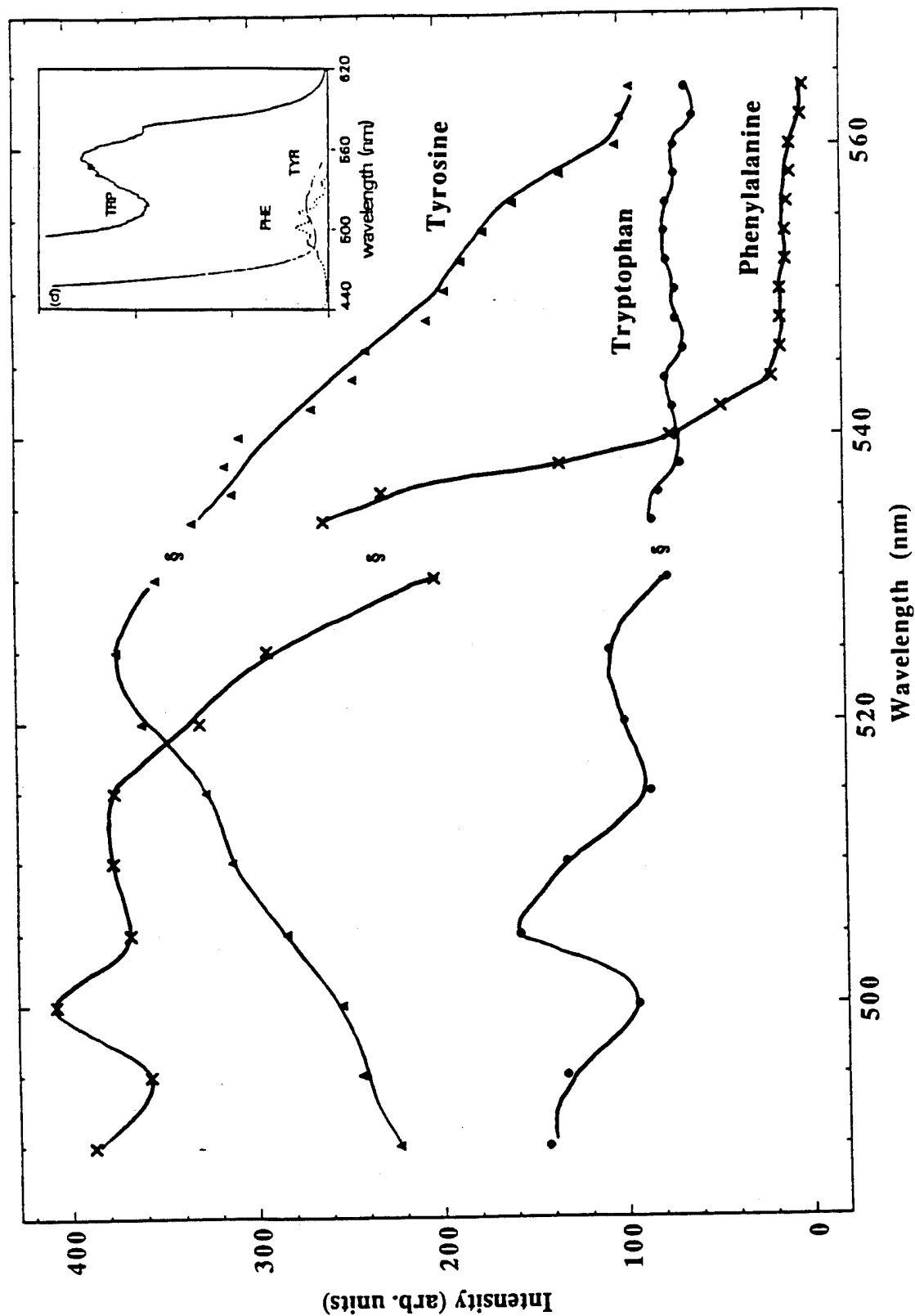**Figure 7.** The TPE of the fluorescence from aqueous solution of tryptophan (dots), tyrosine (triangles), and phenylalanine (crosses), at 10^{-3} M. The incident laser wavelength extends from 396 to 428 nm.

22

2. TPE fluorescences for tyrosine and phenylalanine are stronger than for tryptophan with λ_{inc} in the range 490 to 540 nm.

3. TPE fluorescences from the three amino acids with λ_{inc} in the range of 396 to 428 nm are three to five times more intense than the TPE fluorescence intensity with λ_{inc} in the 490- to 560-nm range.

Working with λ_{inc} in the range 480 to 540 nm may provide more uniqueness for identification purposes. The two-photon fluorescence in this excitation region is strong enough to provide a subpart-per-thousand detectability. By using a solar-blind PMT, we are able to suppress the dominant two-photon fluorescence signal from tryptophan (figure 4d). A solar-blind PMT also has the added advantage of rejection of background radiation for remote sensing applications.

3.2   Two-Photon Induced Lasing in Droplets

3.2.1   Introduction

Various third-order nonlinear optical effects were observed in micrometer-size droplets. [12,13] The front surface of a droplet acts as a thick lens to enhance the internal intensity of the input laser radiation, and the spherical shape of the droplet acts as an optical cavity to provide feedback at specific wavelengths corresponding to morphology dependent resonances (MDRs). The two effects together greatly reduce the input laser intensity required to observe various nonlinear optical effects.

Lasing can occur in droplets of laser dye solutions pumped by either a continuous wave or a pulsed laser. [14,15,16] It has been shown that the lasing threshold is further decreased because of the gain enhancement through cavity QED effects. [17] In all the previous observations of lasing in microdroplets, the upper lasing transition is pumped by OPA to the first excited band of the dye molecule. Upconversion of semiconductor diode lasers has been studied recently for their potential applicability as an all solid state source with a wavelength span from UV to red. [18]

In this work, we observe lasing when the dye molecules are pumped by TPA in various coumarin and rhodamine 6G (R6G) dyes. We compare the first or second excited bands of R6G, and we discuss some of the potential problems encountered at the high-pump laser intensity required for two-photon pumped lasing.

3.2.2 *Experimental Results*

In our experiments, we used a modified Berglund-Liu vibrating orifice droplet generator to produce a stream of monodispersed ethanol droplets (with radii about 50 μm) containing fluorescent dyes of various concentrations. The various lasers used to pump the droplets by TPA are synchronously triggered by the frequency generator that drives the droplet generator orifice at about 50 kHz. The TPA induced lasing emission from the dye doped ethanol droplets is collected at 90° to the incident laser beam and is imaged onto the entrance slit of a spectrograph (Spex Singlemate model 1870). At the exit plane of the spectrograph, a charge coupled device detector is used for the coumarin doped droplet measurements; whereas, a red-enhanced intensified linear photodiode array detector is used for the R6G doped droplet measurements.

Two photon pumping of coumarin doped ethanol droplets is studied with the Stokes shifted emission (at 629.6 nm) of a methane-gas Raman cell pumped by the second harmonic (532 nm) of a Q-switched Nd:YAG laser. To our knowledge, there are no detailed TPA studies in coumarin dyes. TPA of the 629.6-nm photons causes an electronic transition to the tail of the first excited electronic band usually reached by OPA. Figure 8 shows a lasing spectrum (integrated over 100 laser shots) of 10^{-2} M coumarin 460 droplets pumped by input radiation at 629.6 nm with an intensity of 1 GW/cm^2. The lasing emission in the 455- to 460-nm region exhibits a distinct set of MDRs (with nearly equal wavelength spacing). Another set of MDRs (with weaker intensity), corresponding to MDRs of a different mode order, occasionally can be observed in the coumarin 460 lasing spectrum. The high dye concentration can cause dimer formation and subsequent fluorescence quenching. However, when the dye concentration is reduced to below 10^{-2} M, lasing cannot be detected.

Figure 8. TPA pumped lasing spectrum of 10^{-2} M coumarin 460 in ethanol droplets with an input laser at 629.6 nm and an input intensity of 1 GW/cm^2. The periodic peaks correspond to the MDR

There have been extensive TPA studies of R6G in bulk solutions. [19,20,21,22] Figure 9 shows the different excitation processes into the various energy bands of R6G. In all previous experiments involving lasing droplets, the single pump-photon energy lies within the strong absorption band of the first excited singlet band (labeled S_1 in figure 9a). The OPA molar absorption coefficient [23] into the S_1 band is approximately 10^5 M^{-1} cm^{-1}. An R6G concentration of 10^{-4} to 10^{-5} M with an absorption coefficient $\alpha = 1$ to 10 cm^{-1} provides enough gain for lasing with OPA pumping. The OPA spectrum [23] of R6G also has a weaker absorption peak at 350 nm associated with the second excited singlet band (labeled S_2 in figure 9b). The OPA molar absorption coefficient into the S_2 band is approximately 10^4 M^{-1} cm^{-1}. After excitation into the S_2 band, the electrons rapidly decay nonradiatively to the S_1 band. Radiative decay from the S_1 band to the ground state has near unity quantum efficiency. TPA from the ground state into the S_1 or S_2 band (figures 9c and 9d) is also well studied, [19] and it has been found that the TPA coefficient of the S_2 band is 30 times that of the S_1 band.

Two-photon pumping of electrons into the S_1 band of R6G dissolved in ethanol (figure 9c) is achieved with a Q-switched multimode Nd:YAG laser with emission wavelength λ_{inc}=1064 nm. Figure 10 shows the TPA induced emission spectrum from ethanol droplets (α = 50 μm) containing 2.5 x 10^{-4} M R6G at several input laser intensities (I_{in}). Because the laser induced breakdown (LIB) threshold is higher in the near infrared than in the visible, higher input laser intensities at 1064 nm can be used to irradiate the droplets without total LIB related droplet destruction. At I_{in} = 5 GW/cm^2, only fluorescence is detected. At I_{in} = 9 GW/cm^2, the MDR related peaks and a sharp increase in the output intensity are indicative of the onset of lasing. Although the plasma continuum is not so evident, the LIB generated plasma can introduce absorption and scattering losses. [24]

With R6G in an optical cell, lasing from the S_1 band has been observed with TPE into the S_2 band by radiation from a Q-switched ruby laser (694.3 nm). [20] Although the TPA is to the S_2 band, rapid nonradiative decay occurs, and the radiative transition is from the S_1 band. The excimer pumped dye laser (operating at 697 nm with Exciton dye LDS 698) is used to study two-photon pumping into the S_2 band of R6G in ethanol droplets (figure 9d).
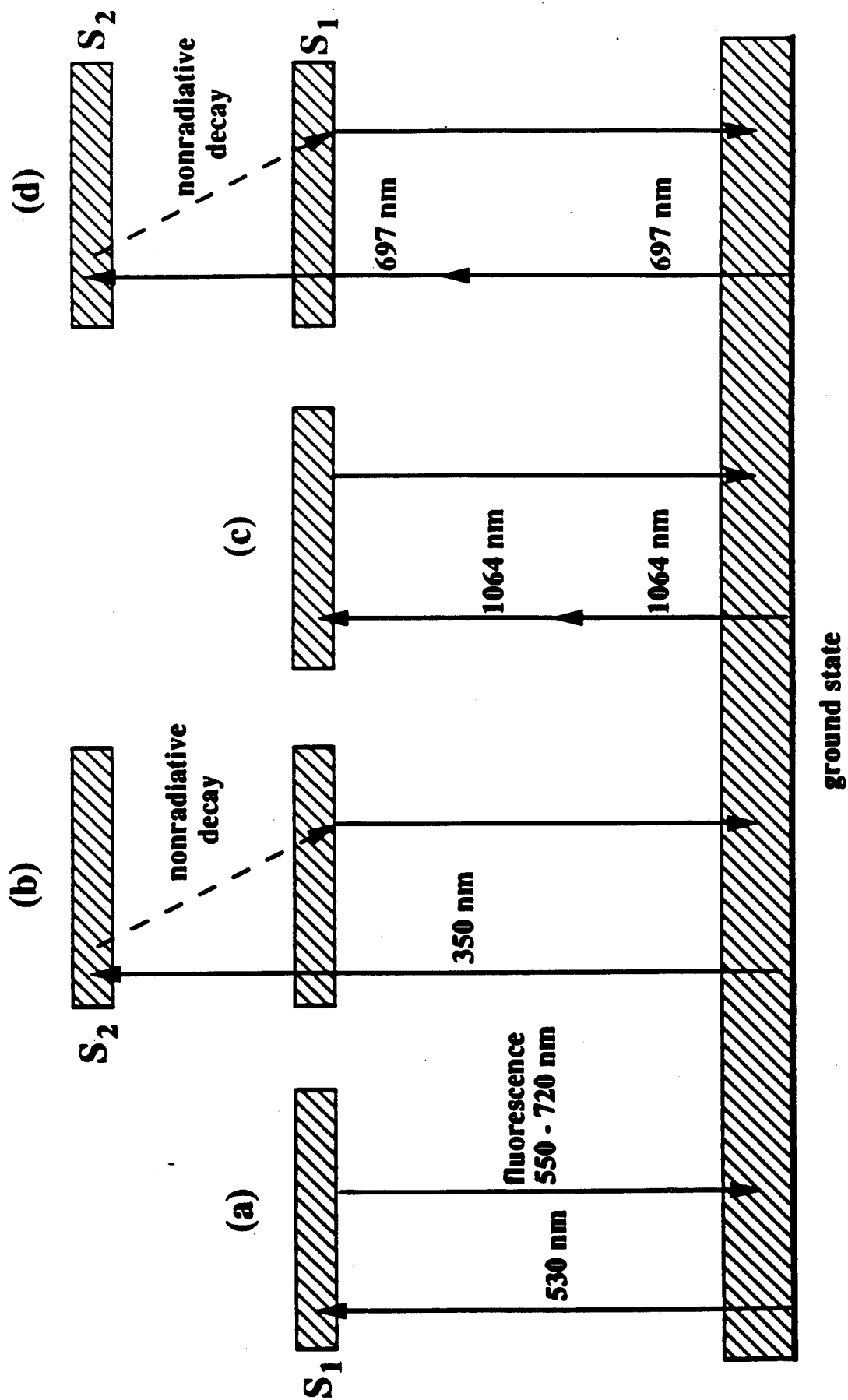
Figure 9. Energy level diagram of R6G under various excitation schemes.
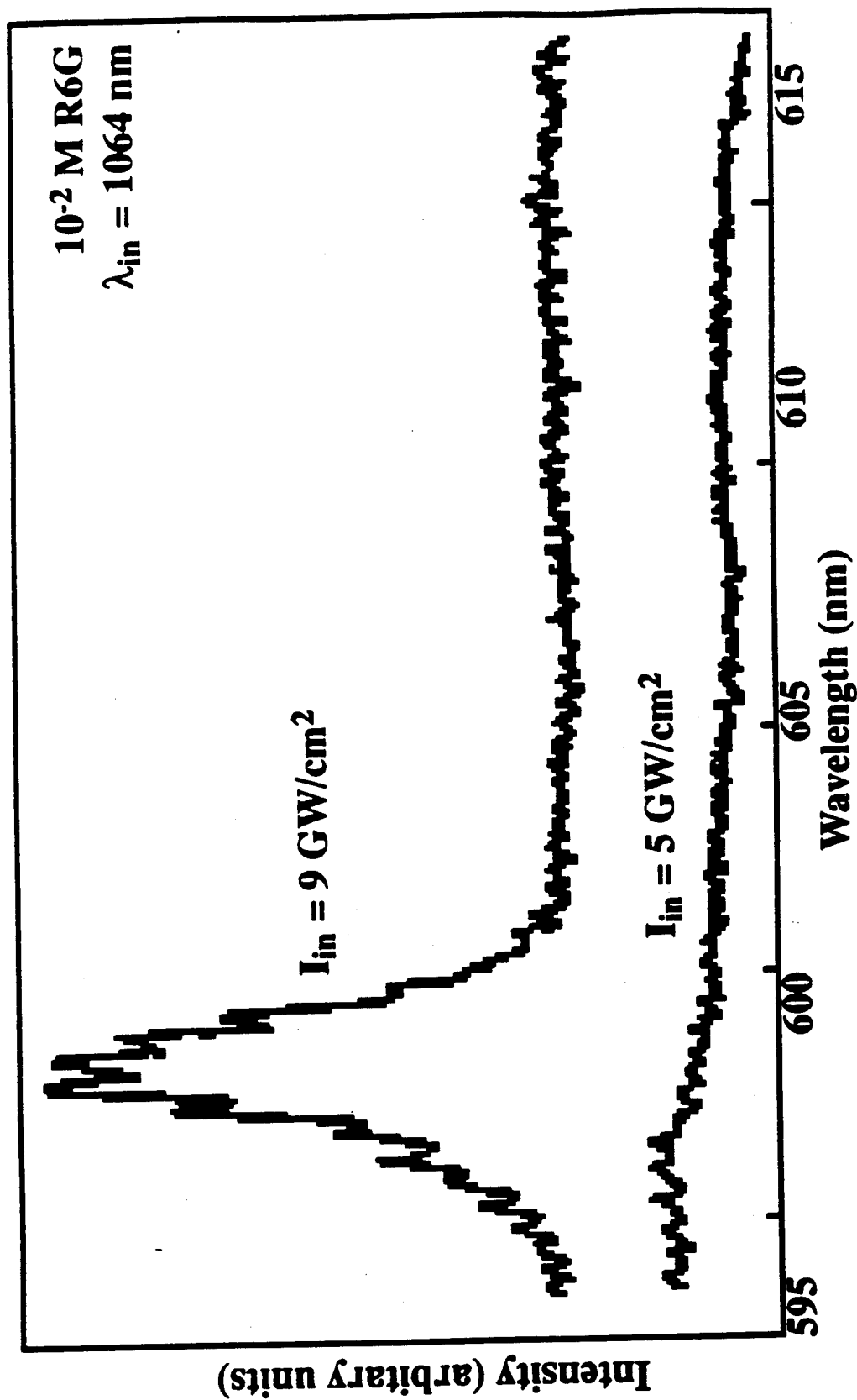
Figure 10. TPA pumped fluorescence and lasing spectrum of 2.5×10^{-4} M R6G in ethanol droplets with input laser at 1064 nm. At 5 GW/cm^2, only fluorescence is detected. At 9 GW/cm^2, MDR related lasing peaks can be observed.

Figure 11 shows the lasing spectrum of 10^{-3} M R6G doped ethanol droplets (α = 50 μm) illuminated at λ_{inc} = 697 nm with I_{in} = 1 GW/cm^2. This input intensity is just below the LIB threshold for λ_{inc} = 697 nm. The lasing spectrum in figure 11 contains a set of well defined MDR related peaks. The lasing spectrum is red shifted because of the increase in absorption caused by the higher dye concentration used (compared with figure 10). The R6G emission signal is weak, and the spectrum shown in figure 11 is obtained with an integration of 170 laser shots with a laser repetition rate of 15 Hz. The MDR related peaks in the lasing spectrum can be broadened by the variation in the droplet size and possible LIB generated plasma. During the experiment, the droplets were viewed through a microscope while they were irradiated by the laser. We observed bright arcs around the rim of the droplet. The arcs are a characteristic feature of lasing droplets. When the R6G concentration is further reduced to 10^{-4} M, no lasing spectrum can be detected at I_{in} below the LIB threshold of the droplets.

Although the droplet morphology provides increased internal input laser intensity, optical feedback, and cavity QED gain enhancement, the input laser intensity needed to invert the electron population with TPA pumping can cause other competing nonlinear optical effects. Stimulated Raman scattering (SRS) is a phase matched third-order nonlinear process readily observable in ethanol droplets. [13] The Raman gain coefficient [25] for ethanol at 694.3 nm is g = 1.3 cm/GW and is larger than the degenerate TPA absorption coefficient β = 0.0075 cm/GW (for 10^{-3} R6G in ethanol) that involves two input laser photons at 694.3 nm. In the case of one pumped photon lasing excitation of 10^{-4} M R6G in ethanol droplets with $I_{in} \approx$ 0.1 GW/cm^2, the Raman gain $G = gI_{in}$ (at the internal high intensity spot) is small, and consequentially, the SRS signal is much weaker than the lasing signal. [15] However, in the case of two-photon pumped lasing excitation, which requires that $I_{in} \approx$ 1 GW/cm^2, the Raman gain (at the internal high intensity spot) is large. With a red enhanced intensified linear array, we observed that the SRS output from ethanol at 875 nm (2928 cm^{-1} Stokes shifted from λ_{inc} = 697 nm) is two to three orders of magnitude larger than the lasing signal. Because the Raman gain is larger than the lasing gain induced by TPA at I_{in} = 1 GW/cm^2, the growth of SRS occurs sooner than the growth of the lasing. Consequentially, the intense SRS
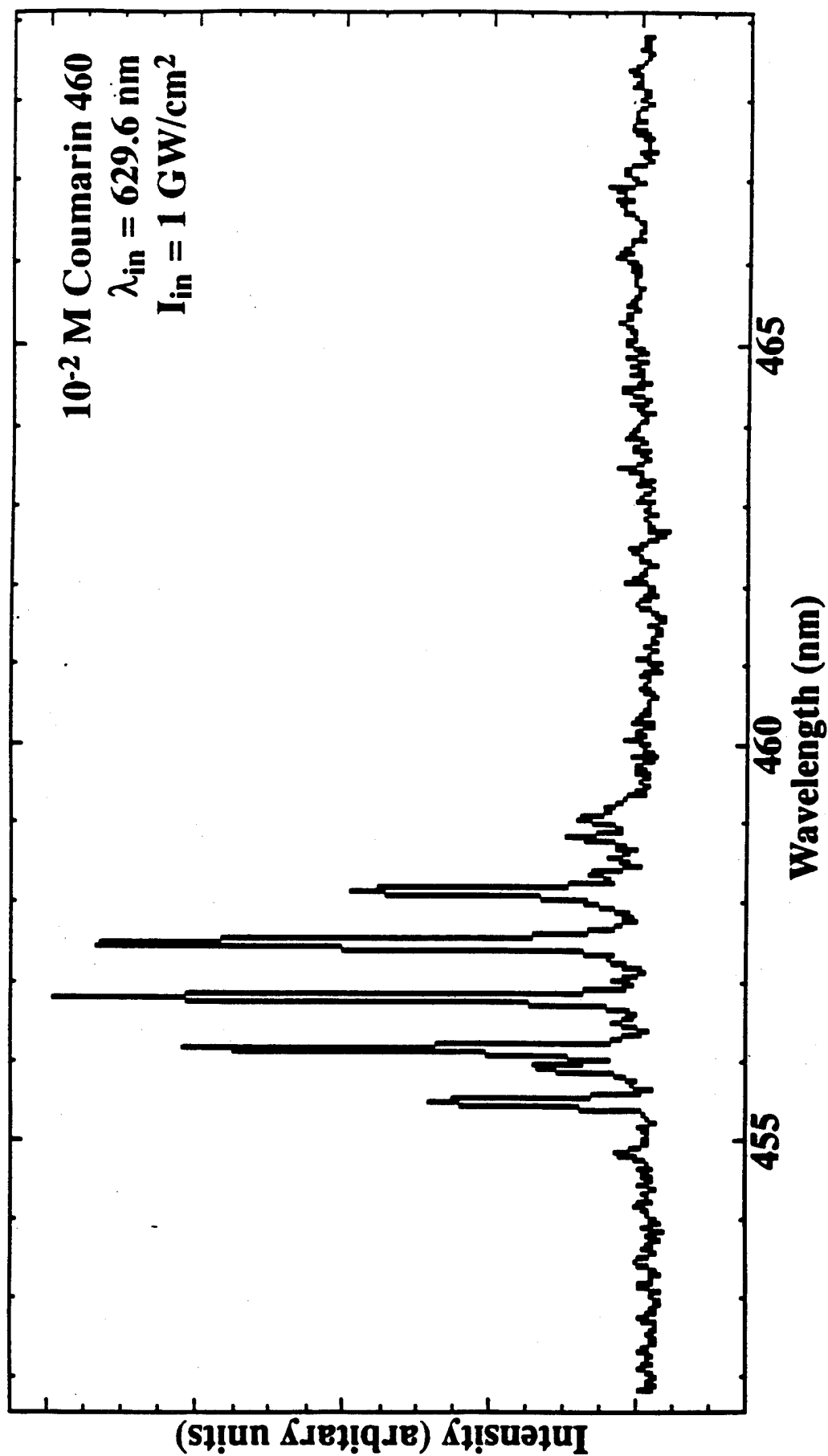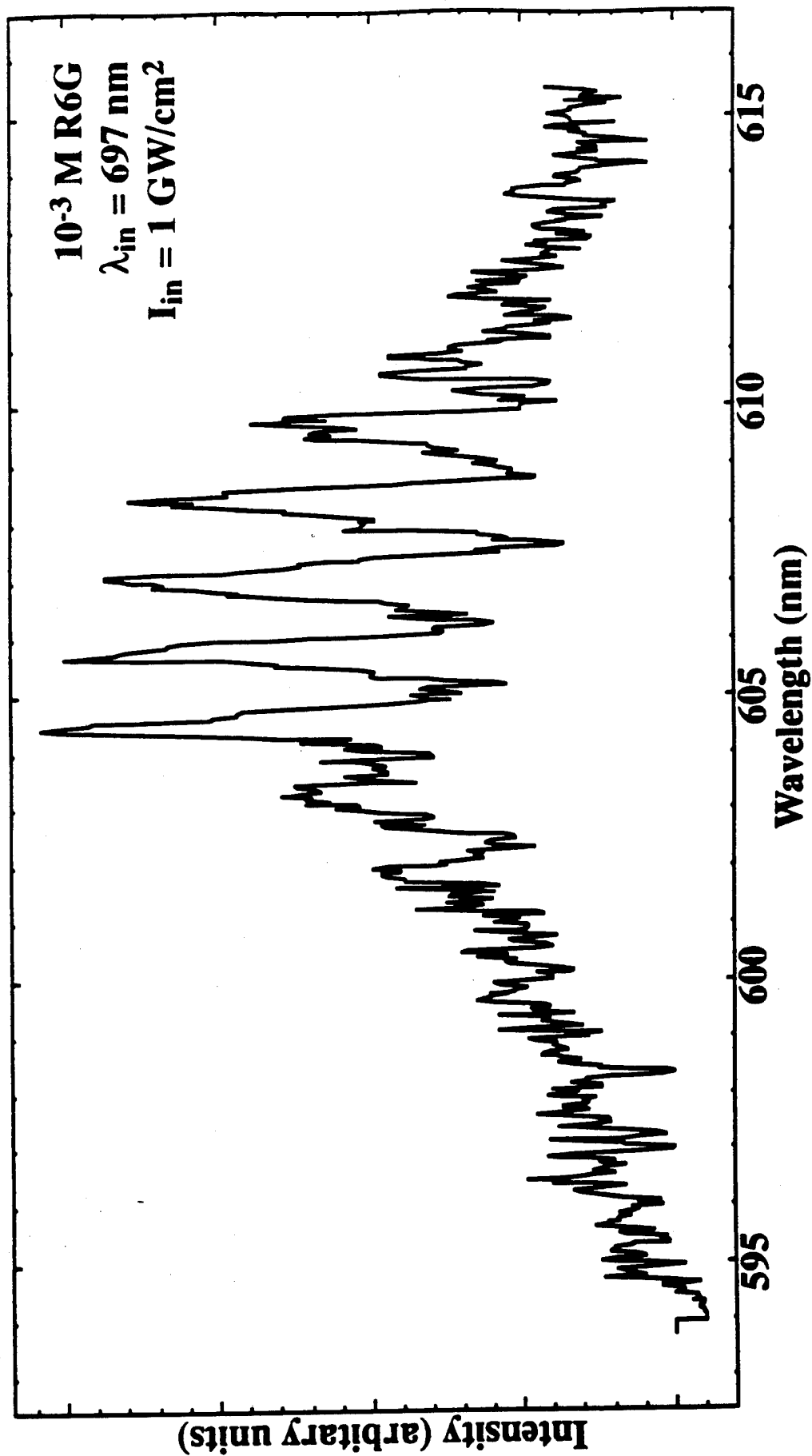
Figure 11. TPA pumped lasing spectrum of 10^{-3} M R6G in ethanol droplets with an input laser at 697 nm and an intensity of 1 GW/cm².

30

can deplete the input laser intensity. When λ_{inc}=1064 nm, competition from SRS is not so severe because the O-H vibrational overtones of water and ethanol molecules absorb the first order Stokes SRS and prevent further growth of SRS in the near infrared. The TPA induced lasing signal can be observed with a concentration of only 2.5 x 10^{-4} M R6G at λ_{inc} = 1064 nm (figure 9c); although, the TPA coefficient of the S_1 band is smaller than that of the S_2 band because there is no SRS competition. As a confirmation, we were not able to observe third harmonic generation or third order sum frequency generation involving the SRS of ethanol and water droplets with λ_{inc} = 1064 nm, which indicates that SRS is too weak or not generated at all in these droplets. [26] Third harmonic generation and third order sum frequency generation were readily observed in D_2O droplets [26] because the O-D vibrational overtones are further in the near infrared; therefore, the SRS intensity can be intense.

There can be other deteriorative factors working against the buildup of lasing intensity at approximately 610 nm in R6G doped ethanol droplets. The first factor is stimulated emission by the input laser at 697 nm. The R6G fluorescence spectrum has a long tail that extends beyond 700 nm, [21] corresponding to transitions from the bottom of the S_1 band to the higher vibrational levels of the ground state. Previous research has shown that the input laser beam at 697 nm can induce stimulated emission [19,22] from the S_1 band and deplete the upper lasing level. Because lasing with R6G-ethanol droplets with TPA of 697-nm photons is observed, the loss by stimulated emission of the input laser is not too deteriorative. The second factor is excited state absorption. Excited state absorption induced by input laser photons a 697 nm and a fluorescent photon at 610 nm can prevent lasing at 610 nm from building up. However, such nondegenerate TPA is not within any electronic bands of R6F and, therefore, it is not important in our experiment.

4. Conclusions

We performed two different experiments to examine the potential of two photon excited fluorescence for detection of biological aerosols: TPE of amino acid droplets and TPE induced lazing of dye doped droplets. Fluorescence spectra with OPE and TPE are the same. However, the fluorescence intensity with TPE is much weaker than that of OPE.

For the amino acid droplet experiment, we observed the following results:

• The fluorescence spectrum of tryptophan is peaked at 348 nm and does not extend to wavelengths below 290 nm.

• The fluorescence spectrum of tyrosine is mainly peaked around 303 nm.

• The phenylalanine is peaked at 282 nm.

• The fluorescence spectra of amino acids alone do not provide much molecular specificity for remote sensing.

TPE potentially offers several advantages for remote sensing of amino acid-containing agents, even though the fluorescence intensity with TPE is much weaker than with OPE: (1) If the first excited state is in the UV or the VUV, atmospheric attenuation of the pump laser radiation can be avoided by using a laser radiation with $1/2 \lambda_{inc}$ to pump with TPE to the same or other excited states. (2) The fluorescence excitation spectrum with TPE may be more specific than that with OPE.

For the dye doped lazing experiment, we made the following observations:

• TPE to certain two-photon allowed excited states can be larger than other two-photon allowed excited states. We used two different excited state energy levels of a rhodamine dye to demonstrate the importance of selecting the optimal two-photon allowed band for TPE.

- In several different types of laser dyes, we have experimentally demonstrated that TPE fluorescence can be intense enough to give rise to lasing in droplets, which because of their spherical morphology can provide a concentration of the internal input pump intensity, feedback, and quantum electrodynamic gain enhancement.

The results of the two experiments allow us to conclude that two photon induced fluorescence is quite weak. It does have the potential to have increased selectivity over regular fluorescence. A primary advantage for this technique is that one can use longer wavelengths for excitation; thus, obtaining greater propagation in the atmosphere. This is particularly true if one must excite at wavelengths substantially shorter than 250 nm.

References

1. Malik, S., cited by D. B. Wetlaufer, "Ultraviolet Sprectra of Preteins and Amino Acids," *Advan. Protein Chem.*, **17**, p 303, 1962.

2. Petruska, J., "Changes in the Electronic Transitions of Aromatic Hydrocarbons on Chemical Substitution," *J. Chem Phys.*, **34**, p 1120, 1961.

3. Eftink, M. R., L. A. Selvidge, P. R. Callis, and A. A. Rehms, "Photophysics of Indole Derivatives: Experimental Resolutions L_a and L_b Transitions and Comparison with Theory," *J. Phys. Chem.*, **94**, p 3469, 1990.

4. Callis, P. R., "Molecular Orbital Theory of the ^1L_b and ^1L_a States of Indole," *J. Chem. Phys.*, **95**, p 4230, 1991.

5. Fasman, G. ed., *CRC Handbook of Biochemistry and Molecular Biology, Vol. I Proteins*, CRC Press, p 183, 1976.

6. Teale, F. W. J., and G. Weber, "Ultraviolet Fluorescence of the Aromatic Amino Acids," *Biochem. J.*, **65**, p 476, 1957.

7. Chen, R. F., "Flourescence Quantum Yields of Tryptophan and Tyrosine," *Anal. Lett.*, **1**, p 35, 1967.

8. Rehms, A. A., S. A. Williams, and P. R. Callis, *Proceedings of the 2nd International Conference on Laser Spectroscopy of Biological Objects*, Pecs, Hungary, p 150-166, 1989.

9. Callis, P., Private communication.

10. Tam, A. C., and C. K. N. Patel, "Two-Photon Absorption Spectra and Cross Section Measurements in Liquids," *Nature*, **280**, p 304, 1979.

11. Callis, P. R., "Two-Photon Properties of the L_a and L_b Bands of Substituted Benzenes Computed for CN DO/S," *Chem. Phy. Lett.*, **107**, p 125, 1984.

12. Qian, S. X., and R. K. Chand, "Multi-Order Strokes Emission from Micrometer-Size Droplets," *Phys. Rev. Lett.*, **56**, p 926, 1986.

13. Acker, W. P., D. H. Leach, and R. K. Chang, "Third-Order Optical Sum-Frequency Generation in Micrometer-Size and Liquid Droplets," *Opt. Lett.*, **14**, p 402, 1989.

14. Tzeng, H. M, K. F. Wall, M. B. Long, and R. K. Chang, *Opt. Lett.*, **9**, p 499, 1984.

15. Biswas, A., H. Latifi, R. L. Armstrong, and R. G. Pinnick, "Time-Resolved Spectroscopy of Laser Emission from Dye-Doped Droplets," *Opt. Lett.*, **14**, p 214, 1989.

16. Lin, H. B., J. D. Eversole, and A. J. Campillo, "Spectral Properties of Lasing Microdroplets," *J. Opt. Soc. Am. B*, **9**, p 43, 1992.

17. Campillo, A. J., J. D. Eversole, and H. B. Lin, "Cavity Quantum Electrodynamic Enhancement of Stimulated Emission in Microdroplets," *Phys Rev. Lett.*, **67**, p 437, 1991.

18. Smart, R. G., D. C. Hanna, A. C. Tropper, S. T. Davey, S. F. Carter, and D. Szebesta, "CW Room Temperature Upconverison Lasing at Blue, Green, and Red Wavelengths in Infrared-Pumped Pr^{3+}-Doped Flouride Fibre," *Electron. Lett.*, **27**, p 1307, 1991.

19. Hermann, J. P., and J. Ducuing, QC 350 0684, *Opt. Commun.*, **6**, p 101, 1972.

20. Topp, M. R., and P. M. Rentzepis, "Picosecond Stimulated Emission in a Flourescent Solution Following Two-Photon Absorption," *Phys. Rev. A*, **3**, p 358, 1971.

21. Bradley, D. J., M. H. R. Hutchinson, H. Koetser, T. Morrow, G. H. C. New, and M. S. Petty, Q41L72, "Interactions of Picosecond Laser Pulses with Organic Molecules," *Proc. R. Soc., London Ser. A*, **328**, p 96, 1972.

22. Sperber, P., and A. Penzkofer, *Opt. Quantum Electron.*, **18**, p 381, 1986.

23. Drexhage, K. H., in "Dye Lasers," *Vol. 1 of Topics in Applied Physics*, ed. F. P. Shafer, Springer-Verlag, New York, p 176, 1989.

24. Hsieh, W. F., J. B. Zheng, and R. K. Chang, "Transmission Through Plasma Crated by Laser-Induced Breakdown of Water Droplets," *Opt. Lett.*, **14**, p 1014, 1989.

25. Wang, C. S., "Quantum Electronics," *Vol. 1: Nonlinear Optics, Part A*, eds. H. Rabin and C. L. Tang, Academic, New York, p 454, 1975.

26. Leach, D. H., W. P. Acker, and R. K. Chang, Effect of the Phase Velocity and Spatial Overlap of Spherical Resources on Sum-Frequency Generation in Droplets," *Opt. Lett.*, **15**, p 895, 1990.

Acronyms and Abbreviations

LIB	laser induced breakdown
MDR	morphology dependent resonance
OPA	one-photon absorption
OPE	one-photon excitation
PMT	photomultiplier tube
R6G	rhodamine 6G
SRS	stimulated Raman scattering
TPA	two-photon absorption
TPE	two-photon excitation
UV	ultraviolet
VUV	vacuum ultraviolet

Distribution

Copies

ARMY CHEMICAL SCHOOL
ATZN CM CC
ATTN MR BARNES
FT MCCLELLAN AL 36205-5020

1

NASA MARSHAL SPACE FLT CTR
ATMOSPHERIC SCIENCES DIV
E501
ATTN DR FICHTL
HUNTSVILLE AL 35802

1

NASA SPACE FLT CTR
ATMOSPHERIC SCIENCES DIV
CODE ED 41 1
HUNTSVILLE AL 35812

1

ARMY STRAT DEFNS CMND
CSSD SL L
ATTN DR LILLY
PO BOX 1500
HUNTSVILLE AL 35807-3801

1

ARMY MISSILE CMND
AMSMI RD AC AD
ATTN DR PETERSON
REDSTONE ARSENAL
AL 35898-5242

1

ARMY MISSILE CMND
AMSMI RD AS SS
ATTN MR H F ANDERSON
REDSTONE ARSENAL
AL 35898-5253

1

ARMY MISSILE CMND
AMSMI RD AS SS
ATTN MR B WILLIAMS
REDSTONE ARSENAL
AL 35898-5253

1

ARMY MISSILE CMND   1
AMSMI RD DE SE
ATTN MR GORDON LILL JR
REDSTONE ARSENAL
AL 35898-5245

ARMY MISSILE CMND   1
REDSTONE SCI INFO CTR
AMSMI RD CS R DOC
REDSTONE ARSENAL
AL 35898-5241

ARMY MISSILE CMND   1
AMSMI
REDSTONE ARSENAL
AL 35898-5253

ARMY INTEL CTR   1
AND FT HUACHUCA
ATSI CDC C
FT HUACHUCA AZ 85613-7000

NORTHROP CORPORATION   1
ELECTR SYST DIV
ATTN MRS T BROHAUGH
2301 W 120TH ST BOX 5032
HAWTHORNE CA 90251-5032

NAVAL WEAPONS CTR   1
CODE 3331
ATTN DR SHLANTA
CHINA LAKE CA 93555

PACIFIC MISSILE TEST CTR   1
GEOPHYSICS DIV
ATTN CODE 3250
POINT MUGU CA 93042-5000

LOCKHEED MIS & SPACE CO   1
ATTN KENNETH R HARDY
ORG 91 01 B 255
3251 HANOVER STREET
PALO ALTO CA 94304-1191

```
NAVAL OCEAN SYST CTR                                    1
CODE 54
ATTN DR RICHTER
SAN DIEGO CA 92152-5000


METEOROLOGIST IN CHARGE                                 1
KWAJALEIN MISSILE RANGE
PO BOX 67
APO SAN FRANCISCO
CA 96555


DEPT OF COMMERCE CTR                                    1
MOUNTAIN ADMINISTRATION
SPPRT CTR LIBRARY R 51
325 S BROADWAY
BOULDER CO 80303


DR HANS J LIEBE                                         1
NTIA ITS S 3
325 S BROADWAY
BOULDER CO 80303


NCAR LIBRARY SERIALS                                    1
NATL CTR FOR ATMOS RSCH
PO BOX 3000
BOULDER CO 80307-3000


DEPT OF COMMERCE CTR                                    1
325 S BROADWAY
BOULDER CO 80303


DAMI POI                                                1
WASH DC 20310-1067


MIL ASST FOR ENV SCI OFC                                1
OF THE UNDERSEC OF DEFNS
FOR RSCH & ENGR R&AT E LS
PENTAGON ROOM 3D129
WASH DC 20301-3080


DEAN RMD                                                1
ATTN DR GOMEZ
WASH DC 20314
```

SPACE NAVAL WARFARE   1
SYST CMND
PMW 145 1G
WASH DC 20362-5100

ARMY INFANTRY   1
ATSH CD CS OR
ATTN DR E DUTOIT
FT BENNING GA 30905-5090

AIR WEATHER SERVICE   1
TECH LIBRARY FL4414 3
SCOTT AFB IL 62225-5458

USAFETAC DNE   1
ATTN MR GLAUBER
SCOTT AFB IL 62225-5008

HQ AWS DOO 1   1
SCOTT AFB IL 62225-5008

ARMY SPACE INSTITUTE   1
ATTN ATZI SI 3
FT LEAVENWORTH
KS 66027-5300

PHILLIPS LABORATORY   1
PL LYP
ATTN MR CHISHOLM
HANSCOM AFB MA 01731-5000

ATMOSPHERIC SCI DIV   1
GEOPHYSICS DIRCTRT
PHILLIPS LABORATORY
HANSCOM AFB MA 01731-5000

PHILLIPS LABORATORY   1
PL LYP 3
HANSCOM AFB MA 01731-5000

RAYTHEON COMPANY   1
ATTN DR SONNENSCHEIN
528 BOSTON POST ROAD
SUDBURY MA 01776
MAIL STOP 1K9

ARMY MATERIEL SYST   1
ANALYSIS ACTIVITY
AMXSY
ATTN MP H COHEN
APG MD 21005-5071

ARMY MATERIEL SYST   1
ANALYSIS ACTIVITY
AMXSY AT
ATTN MR CAMPBELL
APG MD 21005-5071

ARMY MATERIEL SYST   1
ANALYSIS ACTIVITY
AMXSY CR
ATTN MR MARCHET
APG MD 21005-5071

ARL CHEMICAL BIOLOGY   1
NUC EFFECTS DIV
AMSRL SL CO
APG MD 21010-5423

ARMY MATERIEL SYST   1
ANALYSIS ACTIVITY
AMXSY
APG MD 21005-5071

NAVAL RESEARCH LABORATORY   1
CODE 4110
ATTN MR RUHNKE
WASH DC 20375-5000

ARMY MATERIEL SYST   1
ANALYSIS ACTIVITY
AMXSY CS
ATTN MR BRADLEY
APG MD 21005-5071

ARMY RESEARCH LABORATORY   1
AMSRL D
2800 POWDER MILL ROAD
ADELPHI MD 20783-1145

ARMY RESEARCH LABORATORY   1
AMSRL OP SD TP
TECHNICAL PUBLISHING
2800 POWDER MILL ROAD
ADELPHI MD 20783-1145

ARMY RESEARCH LABORATORY   1
AMSRL OP CI SD TL
2800 POWDER MILL ROAD
ADELPHI MD 20783-1145

ARMY RESEARCH LABORATORY   1
AMSRL SS SH
ATTN DR SZTANKAY
2800 POWDER MILL ROAD
ADELPHI MD 20783-1145

ARMY RESEARCH LABORATORY   1
AMSRL
2800 POWDER MILL ROAD
ADELPHI MD 20783-1145

NATIONAL SECURITY AGCY W21   1
ATTN DR LONGBOTHUM
9800 SAVAGE ROAD
FT GEORGE G MEADE
MD 20755-6000

ARMY AVIATION CTR   1
ATZQ D MA
ATTN MR HEATH
FT RUCKER AL 36362

OIC NAVSWC   1
TECH LIBRARY CODE E 232
SILVER SPRINGS
MD 20903-5000

ARMY RSRC OFC   1
ATTN DRXRO GS
PO BOX 12211
RTP NC 27009

DR JERRY DAVIS   1
NCSU
PO BOX 8208
RALEIGH NC 27650-8208

```
ARMY CCREL                                                      1
CECRL GP
ATTN DR DETSCH
HANOVER NH 03755-1290


ARMY ARDEC                                                      1
SMCAR IMI I BLDG 59
DOVER NJ 07806-5000


ARMY SATELLITE COMM AGCY                                        1
DRCPM SC 3
FT MONMOUTH NJ 07703-5303


ARMY COMMUNICATIONS                                             1
ELECTR CTR FOR EW RSTA
AMSEL EW D
FT MONMOUTH NJ 07703-5303


ARMY COMMUNICATIONS                                             1
ELECTR CTR FOR EW RSTA
AMSEL EW MD
FT MONMOUTH NJ 07703-5303


ARMY DUGWAY PROVING GRD                                         1
STEDP MT DA L 3
DUGWAY UT 84022-5000


ARMY DUGWAY PROVING GRD                                         1
STEDP MT M
ATTN MR BOWERS
DUGWAY UT 84022-5000


DEPT OF THE AIR FORCE                                           1
OL A 2D WEATHER SQUAD MAC
HOLLOMAN AFB
NM 88330-5000


PL WE                                                          1
KIRTLAND AFB NM
87118-6008


USAF ROME LAB TECH                                             1
CORRIDOR W STE 262 RL SUL
26 ELECTR PKWY BLD 106
GRIFFISS AFB
NY 13441-4514
```

AFMC DOW   1
WRIGHT PATTERSON AFB
OH 0334-5000

ARMY FIELD ARTLLRY SCHOOL   1
ATSF TSM TA
FT SILL OK 73503-5600

NAVAL AIR DEV CTR   1
CODE 5012
ATTN AL SALIK
WARMINISTER PA 18974

ARMY FOREGN SCI TECH CTR   1
CM
220 7TH STREET NE
CHARLOTTESVILLE
VA 22901-5396

NAVAL SURFACE WEAPONS CTR   1
CODE G63
DAHLGREN VA 22448-5000

ARMY OEC   1
CSTE EFS
PARK CENTER IV
4501 FORD AVE
ALEXANDRIA VA 22302-1458

ARMY CORPS OF ENGRS   1
ENGR TOPOGRAPHICS LAB
ETL GS LB
FT BELVOIR VA 22060

TAC DOWP   1
LANGLEY AFB
VA 23665-5524

ARMY TOPO ENGR CTR   1
CETEC ZC 1
FT BELVOIR VA 22060-5546

LOGISTICS CTR   1
ATCL CE
FT LEE VA 23801-6000

48

SCI AND TECHNOLOGY   1
101 RESEARCH DRIVE
HAMPTON VA 23666-1340

ARMY NUCLEAR CML AGCY   1
MONA ZB BLDG 2073
SPRINGFIELD VA 22150-3198

ARMY FIELD ARTLLRY SCHOOL   1
ATSF F FD
FT SILL OK 73503-5600

USATRADOC   1
ATCD FA
FT MONROE VA 23651-5170

ARMY TRADOC ANALYSIS CTR   1
ATRC WSS R
WSMR NM 88002-5502

ARMY RESEARCH LABORATORY   1
AMSRL BE M
BATTLEFIELD ENVIR DIR
WSMR NM 88002-5501

ARMY RESEARCH LABORATORY   1
AMSRL BE A
BATTLEFIELD ENVIR DIR
WSMR NM 88002-5501

ARMY RESEARCH LABORATORY   1
AMSRL BE W
BATTLEFIELD ENVIR DIR
WSMR NM 88002-5501

ARMY RESEARCH LABORATORY   1
AMSRL BE
ATTN MR VEAZEY
BATTLEFIELD ENVIR DIR
WSMR NM 88002-5501

DEFNS TECH INFO CTR   1
CENTER DTIC BLS
BLDG 5 CAMERON STATION
ALEXANDRIA
VA 22304-6145

ARMY MISSILE CMND   1
AMSMI
REDSTONE ARSENAL
AL 35898-5243

ARMY DUGWAY PROVING GRD   1
STEDP 3
DUGWAY UT 84022-5000

USATRADOC   1
ATCD FA
FT MONROE VA 23651-5170

ARMY FIELD ARTLRY SCHOOL   1
ATSF
FT SILL OK 73503-5600

WSMR TECH LIBRARY BR   1
STEWS IM IT
WSMR NM 88001

Record Copy   10

Total   96